Novel Fluidic Control System for Stacked Rapid Sand Filters

Michael J. Adelman[1]; Monroe L. Weber-Shirk, Ph.D., M.ASCE[2]; Jeffrey C. Will[3]; Anderson N. Cordero[4]; William J. Maher[5]; and Leonard W. Lion, Ph.D.[6]

Abstract: Infrastructure for water treatment faces numerous challenges around the world, including the high failure rate of digital, electronic, pneumatic, and mechanical control systems due to their large number of components and their dependency on proprietary parts for repair. The development of more efficient, reliable, easily repaired water treatment controls that rely on simple fluidics rather than on complex systems has the potential to significantly improve the reliability of drinking water treatment plants, particularly for cities and towns in developing countries. A stacked rapid sand filter (SRSF) has been proposed as a more robust and sustainable alternative to conventional rapid sand filters because each filter can backwash at the same flow rate used for filtration without requiring pumps or storage tanks. While the concept of this filter has been demonstrated in previous studies, this paper presents a novel control system for the SRSF based on fluidics that eliminates the need for mechanized controls. The water level in the filter is regulated by a siphon pipe, which conveys flow during backwash and which contains an air trap to block flow during filtration. The state of the siphon pipe and the ensuing state of the filter are controlled by one small-diameter air valve. This fluidic control system was tested in pilot-scale experiments, which demonstrated its ability to set the mode of operation of the filter and served as the basis for the derivation of design equations. In addition, the first full-size SRSF was built at a municipal water plant in Honduras using this fluidic control system, which provided a full-scale demonstration of its effectiveness. This simple and robust control system shows promise as part of a sustainable rapid sand filtration process. **DOI: 10.1061/(ASCE)EE.1943-7870.0000700.**

CE Database subject headings: Sand filters; Water treatment; Drinking water; Municipal water; Backwashing (water treatment); Sustainable development; Control systems; Flow control.

Author keywords: Sand filter; Water treatment; Drinking water; Municipal water; Backwashing; Sustainable development; Control systems; Flow control.

Introduction

In many cities and towns throughout the developing world, drinking water infrastructure is inadequate, under-performing, or technically deficient (Lee and Schwab 2005). Failure of water treatment systems is part of the reason why an estimated 1.8 billion people lack access to safe drinking water (Onda et al. 2012). Moreover, the high capital and operating costs of water treatment systems have been identified as major barriers to their more widespread implementation in developing countries (Hokanson et al. 2007). In industrialized countries, water treatment systems are more widely available, but there is nevertheless a significant need of capital for maintenance and for new water infrastructure in the coming decades (ASCE 2009).

Water treatment plants that rely on digital, electronic, pneumatic, and mechanized control systems have multiple failure modes that result in a short mean time between repair events. The failures of mechanized plants are due to component failures, reliance on proprietary parts that are unavailable in the local supply chains, high energy costs, and designs that fail to provide adequate feedback to the operator for successful water treatment. For example, 20 modular mechanized water treatment plants were installed in Honduran cities in a program that ended in 2008. By the beginning of 2012, 50% of the plants had been abandoned due to control system failures and significant energy costs (D. W. Smith, personal communication, 2012).

The choice of technology is a crucial factor to achieve sustainability for water projects (Breslin 2003), and the use of technology that is inappropriate for its context is a reason for many failures of infrastructure systems (Moe and Rheingans 2006). Water treatment plants can be designed for sustainable operation and a long useful life by simplifying the control system, eliminating dependence on electricity, minimizing the number of moving parts, designing the unit processes to provide operator feedback, using locally available materials, and simplifying operation and maintenance procedures. Although water treatment plant mechanization and automation might normally be expected to reduce labor requirements and thus operating costs, the need for highly skilled professionals with

[1]Associate Engineer, MWH Global, Inc., 618 Michillinda Ave, Arcadia, CA 91007. E-mail: adelmanmj88@gmail.com

[2]Senior Lecturer/Research Associate, School of Civil and Environmental Engineering, Hollister Hall, Cornell Univ., Ithaca, NY 14853 (corresponding author). E-mail: mw24@cornell.edu

[3]Fulbright Fellow, Agua Para el Pueblo, Tegucigalpa, M.D.C., F.M., 11101 Honduras. E-mail: jeffreywill122@gmail.com

[4]Systems Consultant, Accenture, 1345 Ave. of the Americas, New York, NY 10105. E-mail: anc26@cornell.edu

[5]Assistant Project Manager, Cauldwell Wingate, 380 Lexington Ave., New York, NY 10168. E-mail: wjm96@cornell.edu

[6]Professor, School of Civil and Environmental Engineering, Hollister Hall, Cornell Univ., Ithaca, NY 14853. E-mail: LWL3@cornell.edu

Note. This manuscript was submitted on June 24, 2012; approved on January 29, 2013; published online on January 31, 2013. Discussion period open until December 1, 2013; separate discussions must be submitted for individual papers. This paper is part of the ***Journal of Environmental Engineering***, Vol. 139, No. 7, July 1, 2013. © ASCE, ISSN 0733-9372/2013/7-939-946/$25.00.

different expertise to maintain the control systems of automated plants may actually increase labor costs. In addition, the parts required for automated systems are not readily available in many areas of the world.

The AguaClara stacked rapid sand filter (SRSF) was invented to address the need for a robust, lower cost, high-performing, and sustainable alternative to conventional rapid sand filters (Adelman et al. 2012). The SRSF uses the same flow rate for the filtration and backwash cycles, and it therefore does not require the pumps or elevated storage tanks needed to backwash conventional filters which typically represent around 50% of their capital cost (Kawamura 1975). The SRSF works by placing inlets and outlets made of well-screen pipe within the sand bed, creating multiple layers that filter in parallel but that are backwashed in series. This allows the SRSF to achieve a backwash velocity equal to the number of layers times the filtration velocity with the same flow entering the filter. The typical design ranges of filtration and backwash velocities for rapid sand filtration differ by approximately a factor of six, making six filter layers an efficient configuration. Flow through the bed of a six-layer SRSF during the filtration and backwash cycles is shown in Fig. 1.

The viability of the SRSF was first demonstrated through laboratory studies and a small-scale field demonstration by Adelman et al. (2012), and the first generation full-scale 12 L/s SRSF was built at a water treatment plant in Honduras in 2011 (Will et al. 2012). The initial report of the SRSF by Adelman et al. (2012) discussed the requirement for flow to be provided to the layers of the sand bed as shown in Fig. 1, but no control system was proposed to achieve this. This paper presents a novel system of fluidics to control the SRSF, supported by theoretical analysis, experimental demonstrations, and full-scale implementation. A fluidic system was chosen to eliminate the failure modes associated with electrical, pneumatic, and other mechanized controls. This system consists of inlet and outlet boxes with riser pipes and a siphon with an air valve to control the mode of operation. It is a simple and robust control technique for the SRSF that allows the operator to select the cycle of operation of the filter with a single small-diameter air valve.

Materials and Methods

Pilot-Scale Apparatus

A pilot-scale apparatus (Fig. 2) was developed for laboratory studies of the proposed fluidic control system, starting from the apparatus used by Adelman et al. (2012) for the original proof-of-concept studies. The SRSF in this system was built in a 10.16 cm (4 in.) diameter clear PVC column with six 20 cm layers. The inlet and outlet pipes were 1.27 cm (1/2 in.) PVC with 0.2 mm well-screen slots spaced at 0.318 cm (1/8 in.) provided by Big Foot Mfg. in Cadillac, MI. The sand bed consisted of typical rapid sand filter sand, with an effective size of 0.45 mm and a uniformity coefficient of 1.4 (Ricci Bros. Sand Co., Port Norris, NJ).

Water was applied to this filter at a total flow rate of 5.3 L/min, giving a backwash velocity of 11 mm/s when the flow passed through all layers in series and a filtration velocity of 1.83 mm/s when the flow was divided among the six layers. These values are consistent with typical design values for filtration and backwash velocities in single-media rapid sand filters (Reynolds and Richards 1996). In the pilot-scale system, flow was pumped into the inlet box from the laboratory water system by a centrifugal pump regulated by a flow control valve.

The experimental apparatus also included fluidic controls to set the mode of operation of the SRSF by controlling air entry to and exit from a siphon system. Important components of this fluidic control system are shown in Fig. 2, including an inlet box where water enters the SRSF from upstream processes, an outlet box for filtered water, a backwash siphon, and an air valve. These components regulate the water levels and flow paths during each cycle of operation. Note that there are open water surfaces as shown in Fig. 2 in the inlet box, outlet box, and filter column.

Control of Parameters and Data Acquisition

Raw water for the laboratory apparatus came from a computer-controlled reservoir which blended hot and cold tap water to achieve a room-temperature mix. The target temperature was set to 22.5°C, and the temperature measured for feedback control with an electronic thermistor generally varied between 22°C and 23°C. This prevented excess dissolved gases in the cold tap water from influencing the hydraulics of the system. The tap water came from the Cornell University water system, and had an average pH of 7.7 with roughly 150 mg/L as $CaCO_3$ of hardness and 120 mg/L as $CaCO_3$ of alkalinity (Foote et al. 2012). The only path for water to exit the inlet box is through the filter, so the filtration rate was set by controlling the flow from the pump.

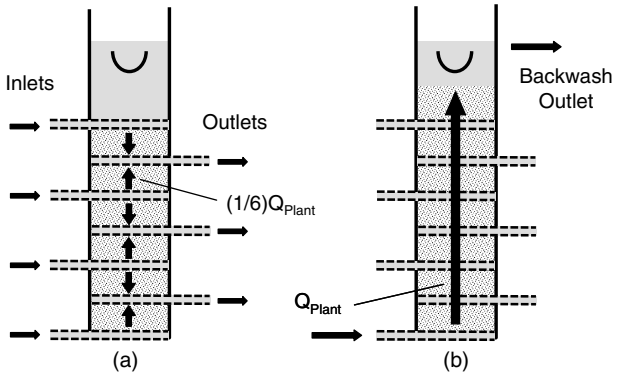

Fig. 1. Diagram of flow in the sand bed of an SRSF during (a) filtration; (b) backwash; the total incoming flow rate Q_{Plant} is the same during both cycles of operation

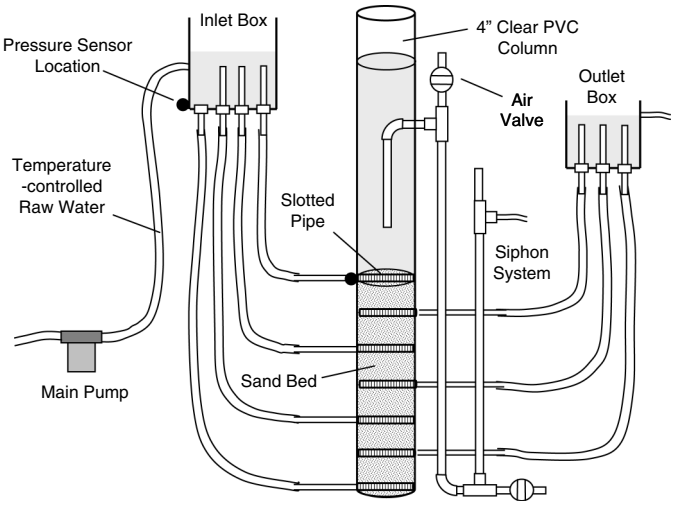

Fig. 2. Pilot-scale experimental apparatus including a SRSF column, inlet and outlet boxes, a backwash siphon, an air valve, and pressure sensors; the water levels shown here are for the filtration cycle

J. Environ. Eng., 2013, 139(7): 939-946

Important water levels in the system were tracked using differential pressure sensors (PX26 series, Omega Engineering Inc., Bridgeport, NJ). These sensors were installed at the locations indicated in Fig. 2, with their positive sides connected via fittings tapped into the walls of the inlet box and filter column, and their negative sides exposed to the atmosphere to establish the baseline for gauge pressure. Because the sensors were installed in vessels with open water surfaces, any pressure they experienced on the positive side was attributable to the height of the water column above them. The sensors were calibrated to measure pressure in units of centimeters of water and zeroed when the open water surface was level with the point where they were tapped through the wall, so that the water level could be tracked in the inlet box and the filter column during experiments. Data from these pressure sensors was logged to a computer via the laboratory process control and data acquisition system described by Weber-Shirk (2009).

Full-Scale Implementation

The first full-scale SRSF was constructed at the municipal water plant serving the town of Támara, Francisco Morazán, Honduras, and came online in October 2011 (Will et al. 2012). This gravity-powered, fully hydraulic 12 L/s facility included existing systems for coagulant dosing, rapid mix, baffled-channel flocculation, upflow sedimentation, and chlorination. The SRSF was installed downstream of the existing sedimentation tanks, and its placement relative to the plant hydraulic grade line allowed flow during both the filtration and backwash cycles to be provided by gravity with no requirement for pumping.

One six-layer SRSF unit in a filter box roughly 1 m by 1.2 m was sufficient to treat the 12 L/s plant flow. It had an active area of 1.1 m^2, giving a filtration velocity of 1.83 mm/s and a backwash velocity of 11 mm/s with the same flow rate. This full-scale SRSF was designed with the sand bed geometry recommended by Adelman et al. (2012) and the fluidic control system described in this paper. It therefore served as a useful full-scale test of all aspects of the SRSF technology.

Results and Discussion

Overall Control System

The SRSF fluidic control system uses the backwash siphon to set the water level in the filter and thereby control the mode of operation (Fig. 3). Only one valve is required to operate this filter—the air valve used to fill or empty the siphon pipe by establishing or releasing an air trap.

When the siphon pipe is blocked by air, the SRSF is in filtration mode. Water is forced to exit over the weir in the outlet box, and the water levels in the inlet box and in the filter are high enough to overcome the filtration head loss HL_{Filter}. This head loss is attributable to flow through the inlet and outlet plumbing, slotted pipes, and sand bed along any one of the six parallel paths through the filter. The clean bed head loss during the filtration cycle can be estimated with familiar models such as the Carmen-Kozeny equation or the Rose equation [see, for example, Reynolds and Richards (1996)].

When there is water flow in the siphon, the SRSF is in backwash mode. The water level in the filter is just high enough for flow to pass through the siphon and exit the system over the backwash weir. The water level in the inlet box drops until it provides the total required backwash head loss HL_{BW}. The head required to fluidize a sand bed is equal to the buoyant weight of the sand, because it represents the force required to suspend the sand grains. Based on both typical properties of filtration sand and on experimental observation, HL_{BW} is approximately equal to the depth of the sand bed in both conventional and stacked rapid sand filters (Adelman et al. 2012). Note that the total backwash head loss also includes losses in the inlet plumbing or siphon pipe. The riser pipes on the entrance to the top three inlets prevent these inlets from receiving flow during backwash, causing all flow to be directed to the bottom inlet in order to fluidize the sand media and backwash the filter.

Experimental Evidence of Mode Transitions

The effectiveness of the fluidic control system to set the mode of operation of the filter was confirmed using the laboratory

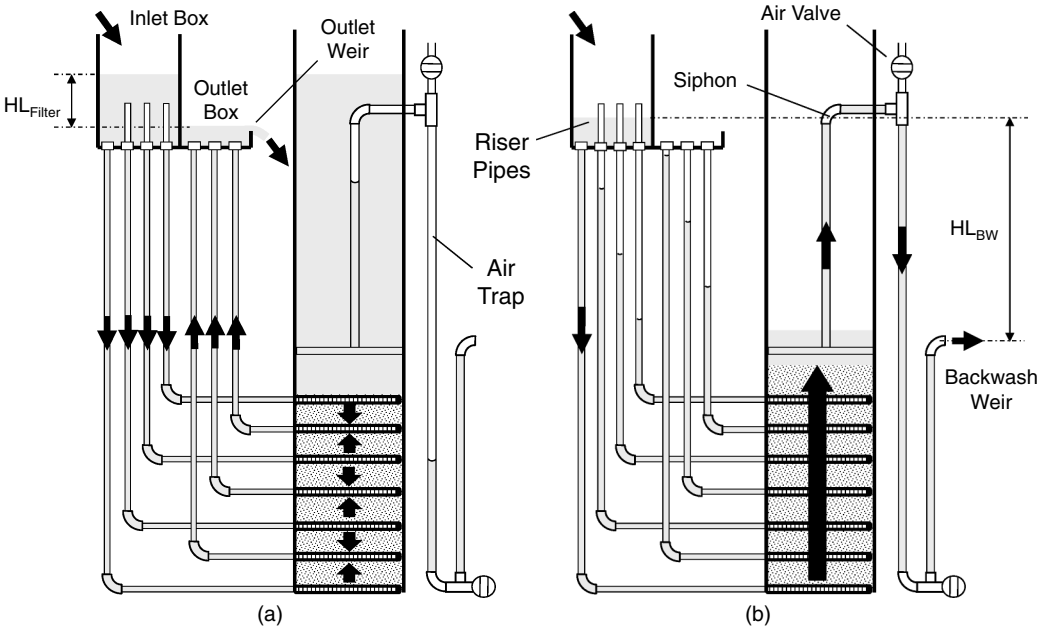

Fig. 3. Fluidic control system for the SRSF, showing water levels during (a) filtration; (b) backwash; important head losses during each cycle are also identified

J. Environ. Eng., 2013, 139(7): 939-946

apparatus. Fig. 4 shows the temporal variation of the water level in the inlet box and the filter column as the control system was used to set both cycles. In the experiment shown, the SRSF started in filtration mode, was changed to backwash, and then was returned to filtration. Water levels in Fig. 4 are measured relative to the top of the settled sand bed.

The data presented in Fig. 4 are divided into five zones illustrating the important steps in the transition between filtration and backwash cycles using the fluidic control system:

1. Zone A;
   - The system is in filtration mode, with the water level high enough in both the inlet box and the filter column for flow to exit over the outlet weir. The inlet box level is a few centimeters above the water level in the filter column, which represents the head loss in the inlet plumbing. The top of the siphon pipe is completely submerged by the water in the filter column, but an air trap is maintained in the siphon to prevent water from escaping to the backwash weir.
2. Zone B;
   - The air valve is opened and then closed over an interval of approximately 5 s. This time interval is also used in the full-scale SRSF. Opening the air valve allows the trapped air to escape, so that the siphon can fill and water can begin flowing out over the backwash weir. Once there is flow in the siphon, the water level quickly drops from its former level above the siphon pipe in both the filter and the inlet box. This transition takes about 1 minute in the laboratory filter and about 3 minutes in the field.
3. Zone C;
   - The system is in backwash mode. The water level in the filter column is a few centimeters above the elevation of the backwash weir, representing the head loss in the siphon pipe. The water level in the inlet box is high enough to provide the 1.2 m backwash head loss (equal to the depth of the sand bed), but below the top of the highest three riser pipes. This directs all flow from the inlet box to the bottom inlet of the filter.
4. Zone D;
   - The air valve is opened and then closed, again for about 5 s in the lab and the field. This allows air to be pulled into the siphon, cutting off flow in the siphon pipe and re-forming the air trap. Because the water can no longer exit via the backwash siphon, it must rise in both the inlet box and the filter column so it can once again exit over the outlet weir. The elevation of the riser pipes in the inlet box is evidenced by the short horizontal section on the trace of the inlet box water level, between about 12 and 14 minutes of run time.
5. Zone E;
   - The system has returned to filtration mode. Once again, the height of water in the filter column reflects the elevation of the outlet weir plus the clean-bed filtration cycle head loss.

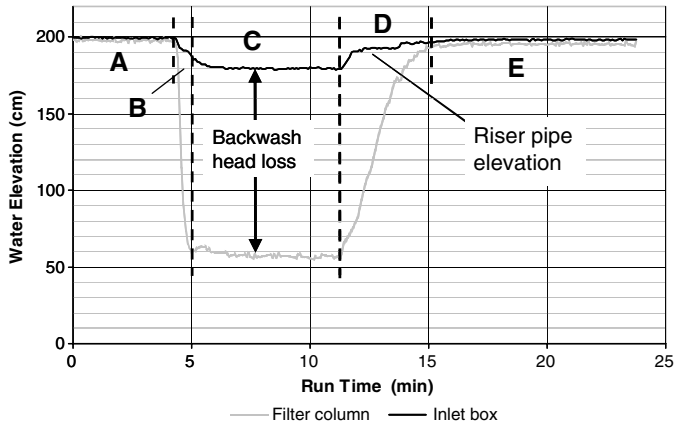

Fig. 4. Water level traces from the pilot-scale apparatus, showing the water level change in the inlet box and the filter column during the transitions between modes of operation; the system starts in filtration mode (Zone A), transitions to backwash (Zone B), backwashes for five minutes (Zone C), transitions back out of backwash (Zone D), and returns to filtration (Zone E)

This data in Fig. 4 provide good evidence that the fluidic control system works as proposed. The effectiveness of this control system was also confirmed by the success of the SRSF in the field. The first full-scale SRSF in Támara can successfully transition between filtration and backwash just as was observed in the pilot-scale system (Will et al. 2012).

Fluidic Control of the Mode of Operation

Controls based on fluidics are used to select which inlets and outlets are active during filtration and backwash modes. Flow to the top three inlets must cease during backwash so that all of the water is forced into the bottom of the filter. The top three inlets are turned off by lowering the water in the inlet box to be below the level of the three inlets, as shown in Fig. 3(b). It is also important that outlet pipes not be hydraulically connected during backwash, to prevent backwash water from preferentially traveling through the pipes instead of through the fluidized sand bed. The outlet pipes are disconnected from each other by lowering the water level in the outlet box to be below the top of the outlet pipes.

The successful transition in flow was based on an analysis to determine the relevant head losses in the system. The placement of the inlet box and the length of the riser pipes depend on both the filtration and backwash cycle head losses. In addition, the energy losses between the entrance to the bottom inlet manifold and the siphon exit can be used to estimate where the water levels will be in the unused inlet and outlet pipes during backwash. The water levels in these pipes are illustrated in Fig. 3(b), and the outlet box must be placed as shown in Fig. 3 to prevent short-circuiting during backwash.

Changes in water levels in the transition from filtration to backwash mode are set by the siphon and controlled by the air valve. To initiate backwash, the air valve opens the siphon pipe, closes three inlet pipes, closes three outlet pipes, and increases the flow rate through the bottom filter inlet. To initiate filtration, the air valve closes the siphon pipe, opens three inlet pipes, and opens three outlet pipes. The use of fluidics thus eliminates seven large-diameter valves—one on each inlet pipe and each outlet pipe—that would otherwise be required to control filter operation.

Backwash Siphon Air Trap Hydrostatics

The siphon pipe and its air trap are the central elements of the SRSF fluidic system, and the design of this siphon pipe is critical to the operation of the control system. The hydrostatics of the SRSF siphon were characterized in the laboratory apparatus. Fig. 5 shows the siphon during backwash mode, the initial air volume that is taken into the pipe just after the air valve is opened to cut off backwash flow, and the hydrostatic equilibrium that is observed during the filtration cycle.

At the end of the backwash cycle, the siphon is broken by opening the air valve. Because the siphon is under negative gauge pressure when it is conveying backwash water, as in Fig. 5(a),

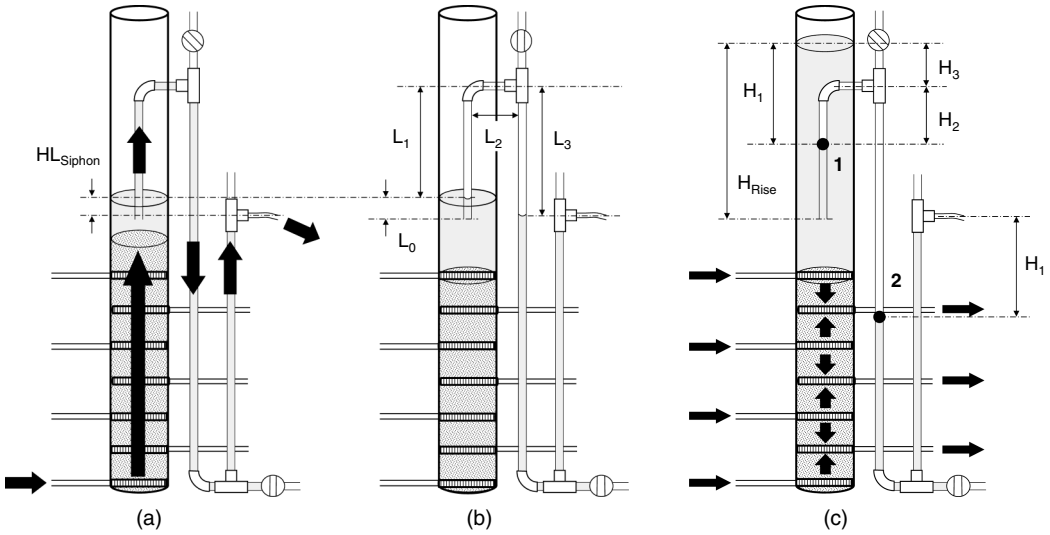

Fig. 5. Diagram of water levels in the siphon pipe and key dimensions (a) during the backwash cycle; (b) just after the siphon is broken to end backwash; (c) after water has risen to the clean-bed filtration height

air will enter the pipe when the air valve is opened. The initial volume of air that is pulled into the siphon pipe at the end of the backwash cycle occupies the lengths L_1, L_2, and L_3 in the siphon pipe, as shown in Fig. 5(b). As the SRSF transitions to filtration mode and the water level rises (Zone D in Fig. 4), this air volume is pushed along the siphon into the position shown in Fig. 5(c).

The siphon pipe geometry must be designed so that the air trap can be maintained as the water level rises in the filter box. The lower U-shaped portion of the siphon pipe remains filled with water that acts as a water seal, and the back pressure on this side of the pipe must be sufficient to resist the pressure exerted on the air trap by the water in the filter column. The density of air is sufficiently small compared to the density of water that the pressure can be assumed to be constant in the air trap, so the hydrostatic pressures at points 1 and 2 in Fig. 5(c) must balance

$$P_1 = P_2 = \rho_{\text{Water}} g H_1 + P_{\text{Atm}} \tag{1}$$

where P_1 and P_2 = absolute pressures at points 1 and 2; P_{Atm} = atmospheric pressure; ρ_{Water} = density of water; g = gravitational acceleration; and H_1 = length defined in Fig. 5(c). Because the pressures balance as shown in Eq. (1), the difference in height from the water in the filter column to point 1 and the vertical displacement of the water seal from the backwash weir to point 2 will have an identical value H_1. The increase in hydrostatic pressure will cause the air in the trap to compress slightly from its initial volume

$$P_{\text{Atm}} V_{\text{Initial}} = P_1 V_{\text{Compressed}} \tag{2}$$

where V_{Initial} = initial air volume; and $V_{\text{Compressed}}$ = volume of the air trap in its compressed state. From the geometry of the system, the initial volume in the air trap is approximately

$$V_{\text{Initial}} = A_{\text{Siphon}}(L_1 + L_2 + L_3) \tag{3}$$

where A_{Siphon} = cross-sectional area of the siphon pipe; and L_1, L_2, and L_3 = pipe lengths defined in Fig. 5(b). Note that this initial air volume is conservatively taken to exclude the length L_0 that remains submerged as a result of the water level in the column during backwash. Once the water has risen in the filter as in Fig. 5(c), the air volume is

$$V_{\text{Compressed}} = A_{\text{Siphon}}(L_2 + L_3 + H_1 + H_2) \tag{4}$$

where H_2 = distance between the water level in the upstream side of the siphon pipe and the horizontal section of the siphon pipe.

The system of Eqs. (1)–(4) can be used to analyze the equilibrium condition in the siphon pipe at any point during filtration. Substituting Eqs. (1), (2), and (4) into Eq. (3) and dividing through by A_{Siphon} gives

$$P_{\text{Atm}}(L_1 + L_2 + L_3) = (\rho_{\text{Water}} g H_1 + P_{\text{Atm}})(L_2 + L_3 + H_1 + H_2) \tag{5}$$

A useful result of Eq. (5) is that it is possible to solve for the position of water levels in the siphon pipe, given the height of water in the filter, H_{Rise}. In order to do this, H_2 is defined geometrically as

$$H_2 = L_0 + L_1 - (H_{\text{Rise}} - H_1) \tag{6}$$

where H_{Rise} = height of water in the filter from the inlet of the siphon pipe. If the water in the column has risen by a given amount H_{Rise}, Eq. (6) can be substituted into Eq. (5) to eliminate all unknowns except for H_1

$$P_{\text{Atm}}(L_1 + L_2 + L_3) = (\rho_{\text{Water}} g H_1 + P_{\text{Atm}})(L_0 + L_1 + L_2 + L_3 + 2H_1 - H_{\text{Rise}}) \tag{7}$$

It is therefore possible to find the position of the water levels on both sides of the siphon pipe by solving for H_1 in Eq. (7).

An important failure mode can also be identified from Eq. (5). When the height of water H_3 over the top of the siphon reaches a certain maximum value, water will begin spilling over into the horizontal section of the siphon pipe. This is the maximum water height that the air trap can support before failing, and it can therefore be used as a design constraint to select an appropriate vertical geometry of the siphon system. This failure mode takes place when the water surface in the siphon pipe just reaches the horizontal segment, so the maximum value of H_3 is found by setting H_2 equal to zero in Eq. (5) and noting that when $H_2 = 0$, H_1 must be equal to $H_{3\text{Max}}$

J. Environ. Eng., 2013, 139(7): 939-946

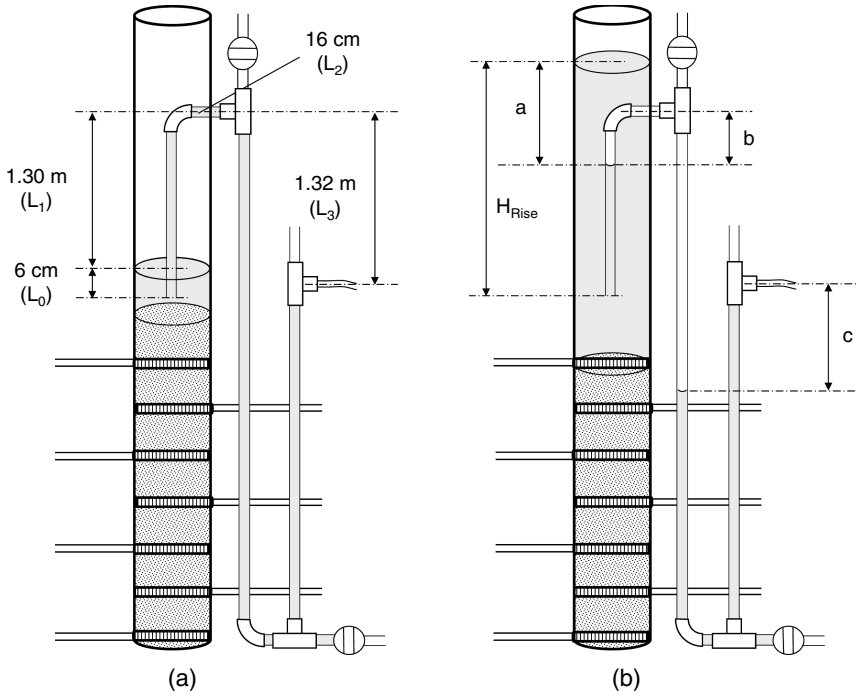

Fig. 6. Diagram of (a) dimensions; (b) observed water levels for the laboratory-scale siphon system; the water in the filter column was allowed to rise a height H_{Rise} over the top of the sand, and the lengths a, b, and c were measured

$$P_{\text{Atm}}(L_1 + L_2 + L_3) = (\rho_{\text{Water}} g H_{3\text{Max}} + P_{\text{Atm}})(L_2 + L_3 + H_{3\text{Max}}) \quad (8)$$

Given the geometry of an SRSF siphon, Eq. (8) can be solved for $H_{3\text{Max}}$, the maximum height of water that the air trap can support during a filtration cycle.

The siphon was evaluated experimentally in laboratory tests to validate this model. Following a backwash cycle, the water was allowed to rise in the column, and the locations of water levels in the siphon system were measured. Dimensions of the experimental siphon and the lengths measured during this experiment are shown in Fig. 6.

For four different heights H_{Rise} of water in the column, the lengths a, b, and c were measured, and Eq. (7) was solved to predict these lengths given the physical dimensions of the siphon in Fig. 6(a). For these calculations, we used the dimensions of the apparatus $L_0 = 6$ cm, $L_1 = 1.30$ m, $L_2 = 16$ cm, and $L_3 = 1.32$ m, and an atmospheric pressure of $P_{\text{Atm}} = 1$ atm. The results of this experiment are shown in Table 1. The measured values of a and c were the same at each point, as predicted by Eq. (1), and the model underestimated the measured values of a, b, and c by 3–6%. The error in the predicted values comes from our estimate of the initial air volume in the siphon pipe—in reality, this initial air volume is larger than the volume shown in Fig. 6(b), because the water passing through the U-shaped tube on the outside of the filter has momentum when the siphon is broken and it is expected to fall below the levels shown in Fig. 6. However, our estimate of the initial air volume represents a minimum value, and it would therefore be appropriate to use the model for a conservative design. This model is conservative because it tends to slightly underestimate the initial volume of the air trap due to inertial effects during filling. A siphon air trap designed with these equations will support a slightly greater depth of water in the filter box than the equations predict.

Table 1. Results of the Siphon Air Trap Hydrostatic Experiments

H_{Rise} (cm)	a (cm)		b (cm)		c (cm)	
	Predicted	Measured	Predicted	Measured	Predicted	Measured
107.8	45.1	47.6	73.2	75.8	45.1	47.6
125.0	52.7	55.2	63.7	66.2	52.7	55.2
142.5	60.6	63.2	54.1	56.7	60.6	63.2
168.0	71.9	74.5	40.0	42.5	71.9	74.5

Note: a, b, and c were predicted from Eq. (7), given H_{Rise}.

Backwash Siphon Air Valve Sizing

The state of operation of the entire system is controlled by the air valve on the backwash siphon. This valve must accomplish two key functions. The first is to allow the air in the siphon air trap to escape when the filter is to be backwashed, as at the beginning of Zone B in Fig. 4. The second is to break the siphon and pull in a new volume of air when backwash is finished and a new filtration cycle is to be started, as in Zone D.

The first function is readily accomplished. When the air valve is opened, the positive gauge pressure on the air trap forces the air to be quickly expelled into the atmosphere. To accomplish the second function, the air valve must allow a sufficient volume of air to enter so that the air trap can be reformed in a reasonable amount of time. The desired flow rate of air to break the siphon and reestablish the air trap therefore sets the minimum required diameter of the air valve. The target air flow rate Q_{Target} of air is based on a desired time t_{Design} to fill the siphon

$$Q_{\text{Target}} = \frac{V_{\text{Initial}}}{T_{\text{Design}}} \quad (9)$$

where V_{Initial} = initial air volume defined in Eq. (1).

In addition to the target flow rate, sizing this valve requires that the relevant driving head and head losses be identified. The initial driving head h_0, measured as a depth of water, is a result of the negative gauge pressure in the upper portion of the siphon during backwash

$$h_0 = \Delta z_{\text{Valve}} + \frac{V_{\text{Siphon}}^2}{2g} + h_{L\text{Siphon}} \quad (10)$$

where Δz_{Valve} = elevation of the air valve tee over the backwash water level in the filter column; V_{Siphon} = flow velocity of water in the siphon; and $h_{L\text{Siphon}}$ = head loss between the siphon entrance and the air valve tee. This equation is dimensionally consistent, as long as all lengths and head losses are expressed in consistent units (e.g., cm of water). When the air valve is initially opened there is a net depth of water h_0 forcing air into the system, but once the siphon pipe is filled with air, the pressure in the pipe approaches 1 atm and the driving head drops to zero. Therefore, the air valve should be designed for an initial flow rate of twice the target flow, because this will produce an average flow of Q_{Target} over a period of t_{Design}, given that the driving head will decline from h_0 to zero. Because minor losses dominate over the short length of the air valve pipe, the minimum size of the air valve D_{Valve} can be calculated by solving the minor loss equation for the diameter of the head loss element

$$D_{\text{Valve}} = \sqrt{\frac{Q_{\text{Design}}}{\pi}} \left(\frac{8K}{g h_{0\text{Air}}} \right)^{1/4} \quad (11)$$

where $Q_{\text{Design}} = 2Q_{\text{Target}}$; the coefficient K incorporates all minor losses along the path of air entering the system, including the air pipe entrance, the air valve itself, the air pipe exit, and any other adaptors or fittings; and $h_{0\text{Air}}$ = initial driving head h_0 from Eq. (10) converted into units of air

$$h_{0\text{Air}} = \left(\frac{\rho_{\text{Water}}}{\rho_{\text{Air}}} \right) h_0 \quad (12)$$

where ρ_{Air} = density of air. The reader is referred to any fluid mechanics textbook for basic formulations of the minor loss equation used to derive Eq. (11) along with tables of typical K values.

In the field, the goal to minimize air valve size was motivated by the desire to reduce construction costs. Using a wood board and hole saws to replicate the orifice size of standard ball valves, a series of tests were performed on the full-scale filter starting with a 7.62 cm (3 in.) PVC ball valve and covering the siphon opening with successively smaller orifices. The tested hole sizes included 5.08 cm (2 in.), 3.81 cm (1.5 in.), 2.54 cm (1 in.), 1.91 cm (3/4 in.), and 1.27 cm (1/2 in.) nominal pipe sizes. Both initiation and breaking of the siphon were tested to ensure that neither transition would fail due to insufficient air leaving or entering the siphon pipe. Successful termination of backwash was defined as having the water from the vertical section of the siphon pipe return to the filter box, indicating that the water in the siphon had been displaced by air.

Observations in the field showed that the air valve could be as small as a 1/2 in. brass ball valve (actual diameter 1.508 cm, or 19/32 in.). No further testing was done with smaller valves, not only because the 1/2 in. valve met the goal of cost reduction and no smaller valve sizes were readily available, but also because the time to initiate and terminate backwash would be unacceptably long for smaller orifice sizes. The full-scale siphon has an air trap volume of approximately 44 L and a fill time of 5.6 s, yielding an average air flow rate of 7.8 L/s. The initial driving head of $h_0 =$ 1.25 m of water for air flow into the full-scale siphon gives a K value of 2.65 in Eq. (11). This is consistent with the nature of the minor losses in the system: the entrance to the air pipe could be thought of as a projecting entrance with $K = 1$, the exit from the air pipe into a much lower velocity zone would have an additional K of 1, and there is some additional minor loss attributable to passage through the ball valve.

Conclusions

A novel system of fluidic controls has been developed for the SRSF to set its mode of operation, and this system has been successfully deployed at a municipal water treatment plant. The fluidic control mechanism is based on a siphon pipe controlled by an air trap, and on water level changes that are designed to automatically engage or disengage three inlets and three outlets. The use of a single small-diameter air valve to fill and empty the siphon with air simplifies operation and completely eliminates all of the failure modes associated with digital, electronic, and pneumatic controls that are common in mechanized water treatment plants. This system is a robust and simple control mechanism for the SRSF that will help make it a sustainable alternative to conventional high-rate filters, particularly for use in the developing world. In addition, the cost of the air control valve is negligible in comparison with conventional digital, electronic, and pneumatic control systems. This novel system was tested in pilot-scale experiments, which demonstrated the transition between the filtration and backwash cycles. Physical models were proposed for the hydrostatics of the siphon air trap and for air flow in the control valve, and these models were validated by observations with the laboratory and full-scale systems.

Acknowledgments

The authors thank Maysoon Sharif, Andrew Hart, Andrew Sargent, Sara Coffey, Min Pang, Ziyao Xu, and Alli Hill at Cornell University for their support of the research and design process, along with Sarah Long, Daniel Smith, Antonio Elvir, Roger Miranda, Jacobo Nuñez, and Arturo Diaz at Agua Para el Pueblo in Tegucigalpa, Honduras for their work on this project in the field. We are also grateful to the members of the Támara municipal Water Board and to water plant operator Antonio Cerrato, who put significant time and resources into the first full-scale SRSF implementation. The laboratory work described in this paper was funded by grants from the U.S. Environmental Protection Agency P3 program, and the construction of the full-scale SRSF was financed by the Sanjuan Foundation and the Támara Water Board.

References

Adelman, M. J., et al. (2012). "Stacked filters: A novel approach to rapid sand filtration." *J. Environ. Eng.*, 138(10), 999–1008.

ASCE. (2009). "2009 Report Card for America's Infrastructure." ⟨http://www.infrastructurereportcard.org/report-cards⟩ (May 24, 2011).

Breslin, E. D. (2003). "The demand-responsive approach in Mozambique: Why choice of technology matters." *UNICEF-Waterfront*, 16, 9–12.

Foote, J., Baker, C., and Bordlemay, C. (2012). "Drinking water quality report." Bolton Point Municipal Water System, City of Ithaca Water System, and Cornell University, ⟨http://www.ci.ithaca.ny.us/departments/dpw/water/report.cfm⟩ (Apr. 8, 2011).

Hokanson, D. R., Zhang, Q., Cowden, J. R., Troschinetz, A. M., Mihelcic, J. R., and Johnson, D. M. (2007). "Challenges to implementing drinking water technologies in developing world countries." *Environ. Eng.: Applied Res. Pract.*, 1, 2–9.

Kawamura, S. (1975). "Design and operation of high-rate filters—Part I." *J. Am. Water Works Assoc.*, 67(10), 535–544.

Lee, E. J., and Schwab, K. J. (2005). "Deficiencies in drinking water distribution systems in developing countries." *J. Water Health*, 3(2), 109–127.

Moe, C. L., and Rheingans, R. D. (2006). "Global challenges in water, sanitation and health." *J. Water Health*, 4(Supp. l), 41–57.

Onda, K., LoBuglio, J., and Bartram, J. (2012). "Global access to safe water: Accounting for water quality and the resulting impact on MDG progress." *Int. J. Environ. Res. Public Health*, 9(3), 880–894.

Reynolds, T. D., and Richards, P. A. (1996). *Unit operations and processes in environmental engineering*, PWS Publishing, Boston.

Weber-Shirk, M. L. (2009). "An automated method for testing process parameters." *Cornell University AguaClara.* ⟨https://confluence.cornell.edu/display/AGUACLARA/Process+Controller+Background⟩ (Jun. 18, 2012).

Will, J. C., Adelman, M. J., Weber-Shirk, M. L., and Lion, L. W. (2012). "Implementation of the AguaClara stacked rapid-sand filtration process at the municipal water treatment plant in Támara, Francisco Morazán, Honduras." *Proc., 27th Congreso Centroamericano de Ingenieria Sanitaria y Ambiental*, Asociación Interamericano de Ingeniería Sanitaria y Ambiental, El Salvador chapter (AIDIS), San Salvador, El Salvador.

J. Environ. Eng., 2013, 139(7): 939-946